Asymmetric Wave Radiation of Oscillating Wedge Buoy

Nonthipat Thaweewat, Surasak Phoemsapthawee* and Sirirat Jungrungruengtaworn

International Maritime College, Kasetsart University, 199 ToongSukhla, Si Racha, Chonburi, Thailand 20230
*Corresponding Author: imcsrp@src.ku.ac.th, Tel. (66)-0-3835-2606, Fax. (66)-0-3835-2607

Abstract

An oscillating body over free surface results wave to radiate. The generated wave form depends on the shape and the movement of the wave generator. In the present study, a heaving asymmetric wedge buoy over free surface is numerically studied via 2D CFD simulations. The numerical results show that wave radiation is also asymmetric related to displacement volume created by the wedge. In this configuration, the propagation of wave energy on inclined wall is relatively enormous compared to the vertical wall. This results in possibility to efficiently harvest wave energy via reverse process of such wave radiation mechanic.

***Keywords**:* Water wave, Wave generator, CFD, VOF, Dynamic mesh

1. Introduction

A wave generator is an essential tool for many naval architecture and offshore tests. It is generally used in order to estimate the wave load and to predict the sea-keeping behavior. The wave form depends on the shape and the movement of the batter of the wave generator. In common, there are two types of batter: the flapping plate and the oscillating wedge buoy.

Y.C. Wu [1] developed a BEM code to study the wave generated by a plunger wedge wave maker. J. Rytkonen and G. Granholm [2] performed an experiment of plunger-type wave maker in a towing tank. In both studies, the wave maker lies at an end of the tank.

Gomes, et al. [3] numerically investigated methods of wave generation in a wave tank using a commercial CFD solver. They compared a moving-plate wave generator with an imposed-velocity-profile Airy wave generator. Wave generator simulations are essentials in many applications especially in offshore design, for an example the study of wave run-up on a square cylinder [4].

Generally, using directly wave generation in reverse process to capture wave energy, for example buoy-type wave energy converters, results in low-to-medium efficiency [5]. This is due to the waves that radiate in every direction from the buoy because of its oscillating motion [6].

The objective of this work is to find a buoy-type wave generator that generate wave in a specific direction and to use such the buoy to capture wave energy via the reverse process. The buoy-type in question is the wedge buoy that is normally installed at an end of the tanks as mentioned before. This paper shows the wave radiation of the wedge buoy when installed at the middle of the free surface.

2. Numerical Method

In this study, a commercial CFD software ANSYS FLUENT V.14 is used to simulate free surface wave generated by a heaving wedge buoy. Based on the mentioned method, the Navier-Stokes equations and the continuity equation are used to describe fluid motion. The flow is transient and incompressible. The viscous model is laminar flow. The Volume of Fluid method (VOF) is used to track and locate the free surface.

2.1 Domain and Boundary Conditions

The 2D computational domain is defined to be 3.1 meter long and 0.6 meter height. The water depth is 0.4 meter shown in Fig. 1. The height and the water depth are corresponding to the physical wave tank of the IMC that is currently used to perform the experiment. The comparable physical investigation will be presented in the future.

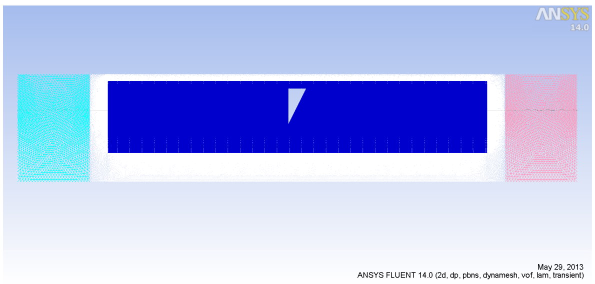

Fig. 1 Computational domain

The asymmetric wedge buoy is right-angled triangle with 0.1 meter width and 0.2 meter height. The tip of the triangle is initially immersed into the water with 0.08 meter depth as shown in Fig. 1.

The top boundary condition is defined to be pressure outlet condition. The no-slip condition of the bottom wall of the domain as well as the wedge walls are satisfied by using wall condition. The right and left walls of the domain are defined as wall condition in combination with porous media zone as suggested by Jungrungruengtaworn and Nontakaew [7] which will be described in the next section. The porous media zones are shown as filled by cyan and pink colors in Fig. 1

2.2. Wave Absorber

Jungrungruengtaworn and Nontakaew [7] have shown that wall condition combined with porous media zone acting as a wave absorber gives qualitative match with the linear wave theory. The mathematic model of the porous media is defined by additional source term S in the Navier-Stokes equations:

$$S = -\left(\frac{\mu}{\alpha} V + C_2 \frac{1}{2} \rho |V| V\right) \tag{1}$$

when

S is additional source term,

V is velocity vector,

$|V|$ is velocity magnitude,

C_2 is inertial resistance factor,

$1/\alpha$ is coefficient of viscous resistance.

As described in Qingjie. Du and Y.C. Dennis. Leung [8], only $1/\alpha$ can be considered. If $1/\alpha$ is too small, the wave energy cannot be effectively absorbed and waves will reflect at the wall. If $1/\alpha$ is too large, the porous media will act as a solid wall and the wave will reflect at the entrance of porous zone. In the present simulation, the coefficient $1/\alpha$ is defined as a function of the position, which is described by a UDF, in order to make the resistance of the porous medium change smoothly as shown in Fig. 2. and Eq. 2

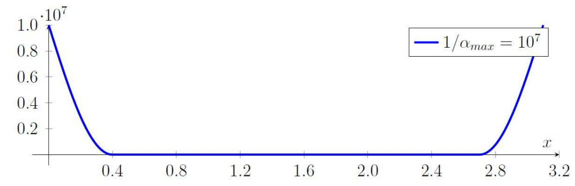

Fig. 2 coefficient of viscous resistance as a function of position described by a UDF

$$\frac{1}{\alpha} = \begin{cases} \left(\frac{1}{\alpha}\right)_{\max}\left(-\cos\left(\left(\frac{0.4-x}{0.8}\right)\pi\right)+1\right) & 0 \le x \le 0.4 \\ 0 & 0.4 < x < 2.7 \\ \left(\frac{1}{\alpha}\right)_{\max}\left(-\cos\left(\left(\frac{x-2.7}{0.8}\right)\pi\right)+1\right) & 2.7 \le x \le 3.1 \end{cases} \quad (2)$$

2.3. Dynamic Mesh

Dynamic mesh is used to prescribe the wedge motion. The surrounding area of the wedge (shown in blue in Fig. 1) is non-reconstruction structure mesh and moving with the wedge. The outer area shown in white in Fig. 1 is unstructured grid and is remeshed every time-step.

The motion of the wedge is prescribed by simple harmonic function:

$$y = A_y(\cos\omega t - 1) \quad (3)$$

when

A_y is motion amplitude,

ω is motion angular velocity,

3. Numerical Results

The free surface behavior and the wave form are numerically studied as a function of the motion amplitude as shown in Table. 1, where ∇ is the displacement volume (m^3), T and f are motion period (s) and frequency ($1/s$) respectively, λ and C are wavelength (m) and wave celerity (m/s) respectively, and a is wave amplitude (m) calculated by linear wave theory which is equivalent to half of wave height $H/2$.

Table. 1 Numerical parameters of the wedge motion to study influence of motion amplitude.

A_y	∇	T	λ	C	a
0.01331	0.00124	0.5	0.39	0.78	0.010
0.01885	0.00186	0.5	0.39	0.78	0.015
0.02391	0.00248	0.5	0.39	0.78	0.020

3.1 Surface Elevation

Fig. 3 shows 2D surface elevation in function of space at the end of the sixth period. The red color represents water phase (VOF=1) while the blue color represents air phase (VOF=0). The water surface is represented by green color which has VOF=0.5.

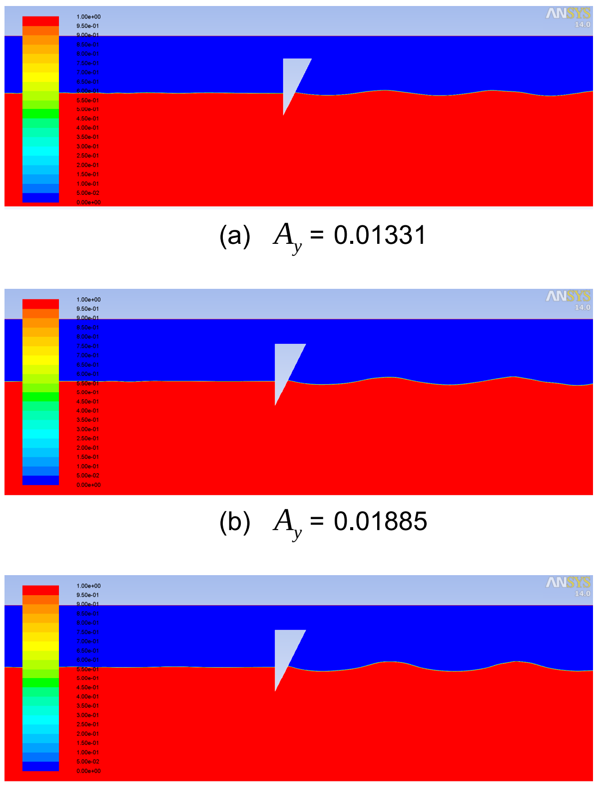

(a) A_y = 0.01331

(b) A_y = 0.01885

(c) A_y = 0.02391

Fig. 3 Surface elevation obtained by VOF method at $t = 6T$.

Fig. 4 shows surface elevation in function of time at $x = \pm\lambda$ from the middle of the wedge. The simulations take approximately 3 periods to become periodic. No wave reflection can visibly be observed that means the porous media effectively absorbs propagated wave energy.

Moreover, the numerical wave amplitudes that propagated to the right (red line) agree well with the linear wave theory (Airy wave). Whereas wave amplitudes that propagated to the left (blue line) is only 10% approximately compared to the right ones. This results in only 1% of wave energy propagation to the left ($P = H^2T$) and therefore can be neglected.

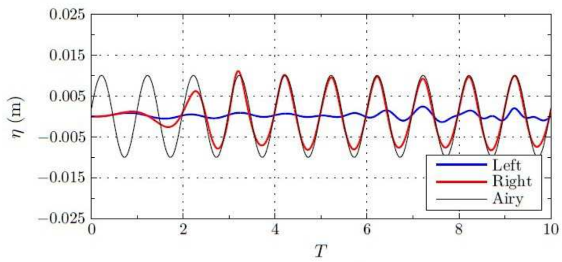

(a) A_y = 0.01331

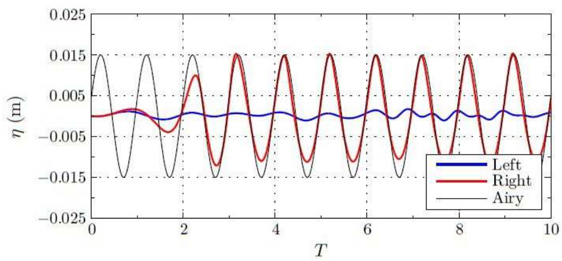

(b) A_y = 0.01885

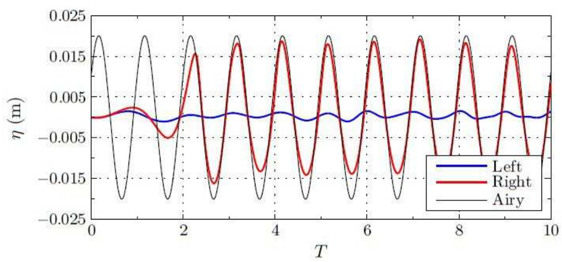

(c) A_y = 0.02391

Fig. 3 Surface elevation in function of time at $x = \pm\lambda$.

This uni-directional wave propagation can be explained by the mean of displacement volume near the free surface. The time dependent surface elevation depends on the rate of change of displacement volume. On the left, there is no displacement volume near the free surface due the vertical wall. Whilst, on the right, the change of displacement volume near the free surface is achieved by the inclined wall of the wedge.

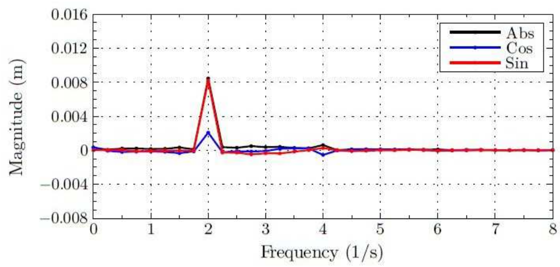

(a) A_y = 0.01331

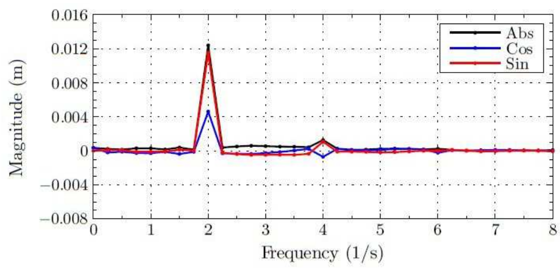

(b) A_y = 0.01885

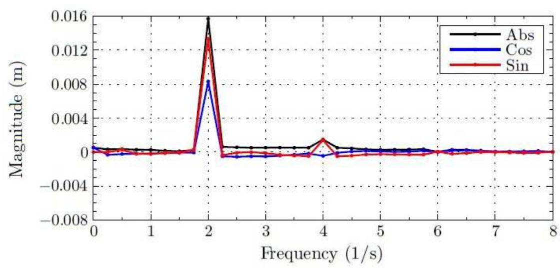

(c) A_y = 0.02391

Fig. 4 Spectral analysis of surface elevation on the right hand side of the wedge at $x = +\lambda$.

This wave generation mechanism of wedge buoy implies possibility to efficiently harvest wave energy via reverse process. Unlike other designs of buoy-type wave energy converter that absorb and radiate wave simultaneously, the wedge buoy wave energy converter should absorb wave energy while the wave radiation is negligible.

3.2 Spectral analysis

Spectral analysis of periodic surface elevation in Fig. 3 is obtained by Fast Fourier Transform, FFT and is presented in Fig. 4.

The analysis shows that the wave is comprised of two components of harmonic wave: the fundamental wave and the secondary wave. The fundamental wave has the same period and hence frequency as the imposed wedge motion. The secondary wave period is half of fundamental period and hence the secondary frequency is twice of the fundamental frequency.

This characteristic can be found in the second-order Stokes wave theory. This higher order wave is influenced by the bottom wall effect.

4. Conclusion

In the present study, the wave generator simulation is modeled using dynamic mesh and VOF method. The wedge motion is prescribed by simple harmonic function.

An asymmetric wave radiation is numerically demonstrated by heaving wedge buoy simulations. The mechanism can be explained by the change of displacement volume near the free surface. The reverse process of such mechanism might be used in wave energy converter in order to achieve great effectiveness.

5. Acknowledgement

The authors would like to thank Energy Policy and Planning Office, Ministry of Energy for financial support.

6. References

[1] Wu, Yung-Chao (1991). Wave generated by a plunger-type wavemaker, *Journal of hydrolics Research*, vol.29, 1991, pp. 851 – 860.

[2] Rytkonen, J. and Granholm, G. (1989). Experimental investigation of the plunger type wave maker, *Rakenteiden Mekaniikka*, vol. 22(3), 1989, pp. 25 – 46.

[3] Gomes, M.N., Isoldi, L.A., Olinto, C.R., Rocha, L.A.O. and Souza, J.A. (2009), Computational Modeling of a Regular Wave Tank, paper presented in *The Third Southern Conference on Computational Modeling (MCSUL) 2009*, pp. 60 – 65.

[4] Repalle, N., Thiagarajan, K. and Paterson, F. (2010). Wave run-up investigation on a square cylinder, paper presented in *The 17th Australasian Fluid Mechanics Conference*, Australia.

[5] Falnes, J. (2002). Ocean waves and oscillating systems, linear interaction including wave-energy extraction, Cambridge University Press, Cambridge, UK.

[6] Lee, Jaw-Fang (1995). On the heave radiation of a rectangular structure, *Journal of Ocean Engineering*, vol. 22(1), 1995, pp. 19 – 34.

[7] Jungrungruengtaworn, Sirirat and Nontakaew, Udomkiat (2012). Two-dimensional Numerical Simulation of Ocean Wave Behavior, paper presented in *the 9th National Kasetsart University Kamphaeng Saen Conference,* Nakhon Pathom, Thailand.

[8] Du, Qingjie and Leung, Y.C. Dennis (2011). 2D Numerical Simulation of Ocean waves, paper presented in *World Renewable Energy Congress,* Linkoping, Sweden.